

AN INVESTIGATION OF HIGH  
VELOCITY AIR FLOW IN A BEND

By

Charles H. Morrison, Jr., Comdr.

USN

R.P.I., Troy, N.Y.      May 1948

Thesis  
M83

Thesis  
M83

Library  
U. S. Naval Postgraduate School,  
Annapolis, Md.

AN INVESTIGATION OF HIGH VELOCITY AIR FLOW  
IN A BEND

by

CHARLES H. MORRISON, JR., COMMANDER,  
UNITED STATES NAVY

Submitted in partial fulfillment of the requirements for  
the degree of Master of Science at Rensselaer Polytechnic  
Institute.

May 1948

#### ACKNOWLEDGMENT

The writer wishes to express his deep appreciation to Professors N. P. Bailey, J. J. Devine, and R. F. Campbell for their assistance and guidance and to Waldo Goyer and his associates of the shop force for their generosity.

## TABLE OF CONTENTS

	<u>Page No.</u>
Summary	
Introduction . . . . .	1
Equipment and Procedure . . . . .	2
Results and Discussion . . . . .	7
Conclusions . . . . .	14
Recommendations . . . . .	15
Bibliography . . . . .	16
 <u>TABLES</u>	 <u>Table No.</u>
Probe Positions on Top Plates . . . . .	I
 <u>FIGURES</u>	 <u>Figure No.</u>
Photograph of Top Plates . . . . .	1
Photograph of Test Equipment . . . . .	2
Schematic of Test Equipment . . . . .	3
Photograph of Probes . . . . .	4
Impact Temperature Correction Curve . . . . .	5
Boundary Layer Flow Pattern . . . . .	6
Total Pressure Versus Radius . . . . .	7
Static Pressure Versus Radius . . . . .	8
Total Temperature Versus Radius . . . . .	9
Velocity Versus Radius . . . . .	10
Weight Flow Per Unit Area Versus Radius . . . . .	11
Total Pressure Variations in the Vertical to Plane of Curvature . . . . .	12
Static Pressure Versus Angular Position . . . . .	13

AN INVESTIGATION OF HIGH VELOCITY AIR FLOW  
IN A BEND

SUMMARY

An investigation of the nature of high velocity air flow in the mid-layer of a 180 degree rectangular cross sectioned bend was made. Total and static pressure and impact temperature traverses were made at 20 degree intervals around the bend. Two zones of flow were found to exist in this layer. The main stream of air, which approximates a free vortex, is progressively moved outward by a turbulent forced vortex extending outward from the inner wall. A negative total temperature gradient extends inward in the forced vortex while total temperature is constant in the free vortex. A method of observing boundary layer flow pattern is described.

## NOMENCLATURE

- A - Cross sectional area.
- "A" - A plane located 1/2" upstream of start of bend.
- "B" - A plane located 1/2" downstream of end of bend.
- g - Acceleration due to gravity, 32.2 ft./sec.<sup>2</sup>
- M - Mach number.
- P - Static pressure.
- P<sub>o</sub> - Total pressure.
- R - Gas constant, 53.3 for air.
- r - Radius to a point in the bend.
- T - Static temperature, °R.
- T<sub>o</sub> - Total temperature, °R.
- v - Velocity, ft./sec.
- W - Fluid weight flow, lbs./sec.
- γ - Ratio of specific heats, 1.395 for air.



# AN INVESTIGATION OF HIGH VELOCITY AIR FLOW IN A BEND

## INTRODUCTION

The purpose of this investigation was to determine the nature of high velocity air flow in a semi-circular bend of a constant, rectangular, cross sectional area, and to see if superacoustic velocities might occur locally on the inner side of the bend.

It is known that low velocity flow in such a bend approaches potential flow with a velocity distribution such that the product of velocity and radius is constant (See reference 1). Subsequent to the laboratory tests, it was found that J. R. Weske, in January of this year (See reference 2) discovered additional relevant information which is discussed later in the report, and that British investigators, in 1943, (See reference 3) observed shock phenomena in similar bends.

A limiting factor in this investigation was an inadequate air supply. Large quantities of air are necessary to produce high velocities in a channel of a size sufficient to permit probing without serious effect on the air flow.



## EQUIPMENT AND PROCEDURE

In addition to the free vortex of the primary flow of low velocity air in a bend, a secondary flow is caused to develop as a result of the high static pressure at the outer radius and the lower static pressure at the inner radius. It consists of two vortices in the cross section plane. These vortices, which are of oppositedirection, converge with parallel velocities outward on either side of the mid-plane of curvature. When the secondary flow is superpositioned with the main stream, the result is two spirals of air proceeding around the bend (See reference 4). This effect can be materially reduced by making the channel deep by comparison to its width.

The ratio of depth to width is known as aspect ratio. According to several authorities, including Patterson, the aspect ratio should be of the order of six to one to get minor secondary flow effects. In this investigation an aspect ratio of one-half was used and the center layer was studied on the premise that it represented the primary flow. A low aspect ratio was necessary because of the restriction of the air supply. Since the cross section had to be in the neighborhood of one-half square inch, a large aspect ratio would necessitate a very small width which is undesirable because of the serious interference of flow by probes.

The bend was designed with a cross section one inch wide and one-half inch deep. The inner radius was one-half inch and the outer radius one and one-half inches. The curved walls of the bend were made of polished wood. Air was brought to the bend through a nozzle designed to produce uniform flow. A one-quarter inch plexiglass plate (Figure 1) was used as the top of the channel while the bottom of the channel was of polished wood. The bend assembly was bolted together so as to be air tight and was in turn bolted through the nozzle flange to a six inch air metering compound which contained a standard A. S. M. E. three-quarter inch metering orifice.

The metering compound was mounted on a lathe bed and piped to the air reservoir. Air, which was supplied by a reciprocating, electric-driven Schramm Compressor, was water cooled. The capacity of the compressor was 0.225 pounds of air per second. (A schematic diagram of the apparatus is shown in Figure 3.)

Three different plexiglass top plates were used, each having holes drilled at different positions (See Table 1). The holes in the plates were tapped to a depth of about .2 inches for a No. 4-40 machine screw. The remaining thickness was drilled with a No. 63 drill (.037" dia.). This hole served as a static pressure tap and as a probe entry for total pressures. It was necessary to redrill these holes with a larger drill in order to insert the thermocouple probe. Initially, the positions of the holes were for a uniform distribution of points in the bend

New holes and additional plates were required later to furnish data on critical positions.

Two types of probes were used, one for impact pressure and one for impact temperature (See Figure 4). They were of such a length that they recorded conditions in the center layer. The pressure probe consisted of a dead-ended No. 20 gage (.032" dia.) hypodermic needle with a No. 80 twist drill (.0135" dia.) hole 0.1" from the end. The needle was soldered to an adapter, the lower part of which was threaded to fit the holes drilled in the top plates. This probe gave excellent results when checked against a normal type impact tube.

The impact temperature probe was an iron constantan thermocouple. Two No. 30 gage thread-covered wires were cemented together with Duco cement, then they were pushed through a No. 16 gage (.051" dia.) stainless steel tube and brought out through a cut away section 0.1 inch from the sealed end of the tube. Next, the wires were welded to form a junction, trimmed, and coated with Duco. The opening was filled with Duco cement and the wires were retracted. The cement was faired so as to give minimum resistance and to leave the thermocouple junction standing out in front. The thermocouple was mounted in an adapter, threaded to fit the probe holes in the top plates. A calibration of the thermocouple was made for subsonic velocities (See Figure 5).

Static pressures were picked up by using an adapter similar to those used for the probes. These static pressures were at the plate and were assumed to be the same as the static pressures in the center layer. Weske verifies the validity of this assumption in reference 2. Spot checks were made through the large holes of Plate No. 3 (See Figure 1) with the Ser's disc used by Vickrey in his work (See reference 5). The assumption was verified within close limits.

Mercury manometers were used throughout for pressure measurements.

Impact temperatures in the metering chamber were obtained using an iron constantan thermocouple, while in the bend the probe described above was used. Ice bath cold junctions were used for both thermocouples. A Brown test potentiometer with connections for two thermocouples was used to measure the voltages generated. The galvanometer was observed through a machinists' magnifying lens. Readings were considered accurate to  $\pm 0.01$  millivolts or  $\pm 0.3^{\circ}$  F.

Pressure readings across the metering nozzle were taken to determine weight flow.

In order to obtain the maximum air supply, all readings were taken with the metering chamber pressure equal to twenty-seven inches of mercury, gage. By getting a surge of air from the reservoir, when pumped up nearly to the setting of the safety valve, and at the same time operating the compressor,



this pressure could be maintained for a reasonable time. The compressor alone would furnish air such that  $P_2$ , the metering chamber pressure, settled at 17.5 inches gage. The total temperature of the incoming air was maintained in the vicinity of  $87^{\circ}$  F.

Initially, pressure readings were taken using Plate No. 1 and  $P_2$  at 18.0 inches of mercury. It was found advisable to go to the higher chamber pressure in order to realize higher velocities in the bend. Unfortunately, the probe holes in Plate No. 1 were too large and irregular to give satisfactory static pressures. Static pressure readings were then taken from Plates No. 2 and 3. Temperature readings were taken using Plate No. 1 only because it was not desirable to redrill the holes of Plates No. 2 and 3 to accommodate the thermocouple probe.

It was noticed at an early stage that the oil particles suspended in the air formed a boundary layer flow pattern on the top plate. In fact, oil particles in the second lamina from the plexiglass could be seen moving at much greater velocities. This pattern was not distinct enough to be photographed. By the addition of small amounts of water to the metering chamber, a milky emulsion of oil, air and water was formed. This emulsion made the pattern readily visible, as shown in Figure 6.

## RESULTS AND DISCUSSION

Static pressure, total pressure, and total temperature found at the different probe positions in the bend appear in the curves of Figures 7, 8, and 9.

The Mach number at each position was determined from the ratio of impact to static pressure by using Curves 2 and 11 of reference 6. Velocity was determined by using Curve 1 of reference 6. Velocity at each probe position appears in the curves of Figure 10. It is to be noted that a free vortex, in which the product of velocity and radius is constant, is highly developed at  $60^\circ$ . The maximum recorded velocity was at radius 0.54",  $60^\circ$  around the bend. The Mach number at this point was 1.376. At  $80^\circ$  around the bend, the velocity at the inner probe position began to fall off. The velocity profile near the inner radius approaches that of a forced vortex in which velocity is proportioned to radius. The transition from free to forced vortex progressively moves outward as the flow continues around the bend, until at point "B" it is located nearly half way across the channel. Supersonic velocities occur in the vicinity of transition from 40 to 160 degrees around the bend.

Curves of weight flow per unit area versus radius (See Figure 11) indicate the nature of weight flow distribution.

The ordinate of these curves is computed from the weight flow equation of reference 6, namely,

$$\frac{W}{h} = \frac{P}{\sqrt{T_0}} f_4 (M)$$

where,

$$f_4 (M) = M \sqrt{\frac{\gamma g}{R} \left(1 + \frac{\gamma-1}{2} M^2\right)}$$

These curves show that the flow cannot be analyzed by the one dimensional approach since there is a radial component of motion. The mass of air flow moves inward as the bend is approached and then tends to move outward, so that at "B" nearly two-thirds of the air flow is in the outer half of the channel. A check on the continuity of the air flow in the mid-layer was made by graphical integration of the area under the curves of Figure 11. It indicated continuity to 100° around the bend where a minor lessening of air flow commenced so that at "B", one-half inch beyond the bend, two per cent of the original flow had left this layer.

It is important to note the loss of total pressure, which begins near the transition point and progresses inward into the forced vortex. In fact, the velocity distribution in this region is due to the total pressure loss. It can be inferred then that this is a turbulent zone, i. e., some of the total pressure has been lost in turbulence. It is reasoned that the air from the secondary flow entering this region is causing the turbulence. It is possible that some separation



may have occurred since oil did not adhere to the mid-section of the inner wall.

A check of total pressure in the vertical was made at four positions, two in the free vortex zone and two in the forced vortex zone. The results are shown in Figure 12. The curves indicate that the forced vortex zone is smaller next to the top plate than in the mid-plane, and that the spiral motion reaches a maximum near the top plate and is very small in the mid-section.

The total temperature differences obtained and shown in Figure 9 are small. With the exception of a few significant readings, these differences are of the order of the cumulative difference to be expected from errors, and radiation and conduction losses. However, it appears that there is a negative gradient inward in the forced vortex zone. This is in agreement with the findings of Vickery in reference 5. Thermal energy is conducted outward in the forced vortex in an effort to equalize the static temperature. This results in lowered total temperature at the inner radius and a raised total temperature in the vicinity of the transition. The total temperature is nearly constant in the free vortex. This is to be expected since the angular velocities of adjacent stream tubes differ in the free vortex whereas in a true forced vortex they are the same.

From Figure 13 it may be noted that there is a static pressure rise between  $60^\circ$  and  $80^\circ$  in the vicinity of radius 0.6". This is taken as possible evidence of a shock. Proof should be furnished by Schlieren observation.

Young, Green, and Owen, in reference 3, took spark photographs of high speed air flow in rectangular, cross sectioned, right-angled bends. They found evidence of local shocks near the inner radius. Their clearest picture was in a bend of two and one-half inch depth, one and one-half inch width, and a mean radius of three inches. These shocks appeared to be plane rather than angle shocks and of fairly great intensity. It is believed that the picture is distorted by the fact that the position of a shock probably varies with the plane of curvature. The fact that their clearest pictures were in bends of the greatest aspect ratio indicates the optimum would be in a bend of aspect ratio about two and mean radius about one inch. The channel must be wide enough so that the velocity gradient across the channel is large and choking does not occur.

The loss coefficients of Young, et. al, are variations of nondimensional ratios of static pressure loss to initial dynamic pressure and total pressure loss to initial dynamic pressure. Mean static pressures based on two center taps in the top and bottom plates and a tap at each curved wall at the exit were used. Total pressure was computed using this mean static pressure and continuity of flow. The use of this mean pressure appears to be improper since this investigation has shown that weight flow at the exit of the bend is far from evenly distributed.

Their conclusions are that, (1) for a given cross sectional area and radius of the center line of a bend, the most efficient shape for a rectangular cross section at high entry Mach numbers is a square; (2) if the radius of such a bend is fairly gentle (e. g. four inch radius for a two inch square cross section), the increase in bend losses with increase in entry Mach number is small up to the entry Mach number at which the bend chokes; and (3) that losses are constant for increased entry total pressure after choking.

Weske, in reference 2, found the pressure and velocity distribution at the exit of the bend in some sixty-four combinations of pipe bends, shapes curvatures, and Reynolds numbers. All of his work was done at low Mach numbers, none of which were over 0.3. He found three regions of flow, namely, the core, and the eddying zone which correspond to the free and forced vortex found in this investigation, and a peripheral zone which is the zone of flow near the top, bottom and outside boundaries. His conclusions about these regions of flow were as follows:

- (a) In the Core:  $v \times r = \text{constant}$ ; flow is predominantly tangential; radial and vertical velocities are small; total pressure is fairly constant; static pressure in the vertical is nearly constant.

- (b) In the Peripheral Zone: tangential velocity is small; peripheral velocity is large; velocity perpendicular to the wall is negligible.
- (c) In the Eddying Zone: Total pressure is not constant;  $\frac{v}{r}$  is nearly constant; eddying conditions range from a steady twisting to intense random turbulence; separation is uncommon except for cases of very small mean radius to width ratio.

Other conclusions made were that:

- (1) The foremost factor affecting flow in bends is the displacement of air of relatively lower total energy toward the region near the inner wall, thus, accounting for the velocity distribution.
- (2) The shape and proportions of the cross section have minor effects on the flow.
- (3) Instability of the flow near the outer wall of large aspect ratio bends leads to mixing of air of different kinetic energies; with small aspect ratio, the tendency is not so preponderant since low kinetic energy air particles are then more readily displaced toward the inside.
- (4) Pronounced variations of velocity produced by bends decay rapidly in the straight pipe, downstream from a bend, whereas, spiralling motion persists over great distances.



- (5) Reynolds' number has no appreciable effect on the velocity profiles.
- (6) The length of the approach has slight effect on velocity profiles.

Thus, this investigation, as far as it went, confirms the present findings of Weske.

Since the total pressure loss in the forced vortex is the principal cause of losses in a bend, efforts to improve bends must be to reduce the size of this region. Possibly the installation of several thin vanes conforming with the curvature and extending a short distance into the stream from the top and bottom walls would produce this effect. It is reasoned that they would reduce the amount of slow boundary layer air being added to this region and possibly lessen the higher velocity secondary flow entering it.

## CONCLUSIONS

The following conclusions are drawn regarding high velocity air flow in a bend:

- (1) Although the flow is three dimensional, a layer in the mid-plane of curvature may be considered two dimensional.
- (2) A free vortex is formed to a high degree.
- (3) A turbulent zone approaching a forced vortex develops at the inner wall and progressively expands outward as the air proceeds around the bend.
- (4) The principal losses occur in this turbulent zone.
- (5) A negative total temperature gradient inward exists in this forced vortex, whereas, total temperature is constant in the free vortex.
- (6) Transition from free to forced vortex is probably caused by the mixing of primary and secondary flows.
- (7) Local supersonic velocities may exist near the transition from free to forced vortex.
- (8) Evidence of a shock was found.

The pattern of boundary layer air flow may be observed visually through a transparent wall when small amounts of water and oil are added to the air stream.





## RECOMMENDATIONS

It is recommended that:

- (1) Schlieren observations be made of high velocity air flow in a bend.
- (2) Three dimensional traverses be made in a bend fitted with small secondary flow reducer ribs fitted on the flat walls of a rectangular cross sectioned bend.

## BIBLIOGRAPHY

- (1) Binder, R. C., "Fluid Mechanics", Prentice-Hall Inc.,  
New York, 1943, Page 126.
- (2) Weske, J. R., "Experimental Investigation of Velocity  
Distributions Downstream of Single Duct  
Bends", NACA TN No. 1471, January 1948.
- (3) Young, Green, and Owen, "Tests of High Speed Flow in  
Right Angled Pipe Bends of Rectangular  
Cross Section", R and M No. 2066,  
October 1943.
- (4) Patterson, G. N., "Note on the Design of Corners in  
Duct Systems", Aeronautical Research  
Committee, R and M No. 1773, October 1936.
- (5) Vickrey, W. C., Jr., "Vortex Flow in an Actual Gas"-  
M. E. Thesis - R. P. I., May 1948.
- (6) Bailey, Neil P., "The Thermodynamics of Air at High  
Velocities", Journal Inst. of Aero.  
Sciences, Volume II, No. 3, July 1944.

TABLE I  
PROBE POSITIONS ON TOP PLATES

PLATE NO. 1

ANGULAR POSITION	RADIUS (INCHES)				
A (1/2" upstream of bend)	0.60	0.80	1.00	1.20	1.40
10°	0.60	0.85	1.02	1.19	1.36
30°	0.62	0.83	1.01	1.17	1.35
50°	0.66	0.83	1.01	1.18	1.35
70°	0.63	0.82	1.02	1.18	1.35
90°	0.65	0.81	1.00	1.17	1.35
110°	0.62	0.82	1.01	--	1.35
130°	0.62	0.82	1.02	1.20	1.40
140°	0.75	--	--	--	--
150°	0.65	0.85	1.02	1.22	1.42
160°	0.75	--	--	--	--
170°	0.63	0.82	1.02	1.22	1.40
B (1/2" downstream of bend)	0.60	0.80	1.00	1.20	1.40

TABLE I  
(continued)

PLATE NO. 2

ANGULAR POSITION	RADIUS (INCHES)					
0°	0.57	0.76	0.97	1.17		1.37
20°	0.58	0.76	0.97	1.16		1.37
40°	0.57	0.76	0.96	1.16		1.36
60°	0.56	0.76	0.96	1.15		1.35
80°	0.57	0.77	0.97	1.17		1.36
100°	0.58	0.78	0.98	1.17		1.37
120°	0.58	0.78	0.98	1.17		1.37
140°	0.53	0.68	0.89	1.08	1.29	1.47
160°	0.53	0.68	0.88	1.09	1.28	1.47
180°	0.55	0.69	0.89	1.09	1.29	1.47

PLATE NO. 3

ANGULAR POSITION	RADIUS (INCHES)
60°	0.54
80°	0.59
90°	1.00 *
100°	0.65
120°	0.65
140°	0.70 *
160°	0.60
180°	0.80

\*Large hole for Ser's disc.

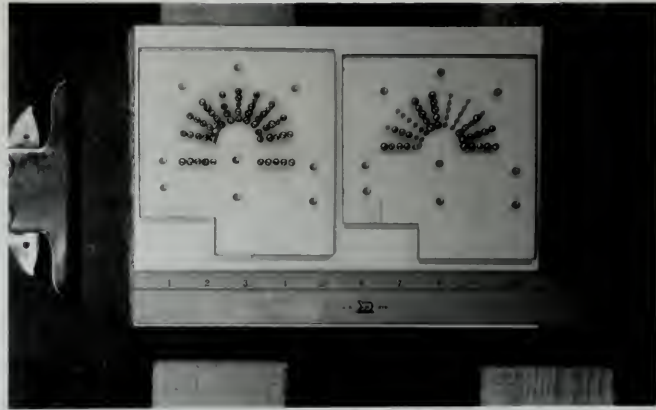


FIGURE 1

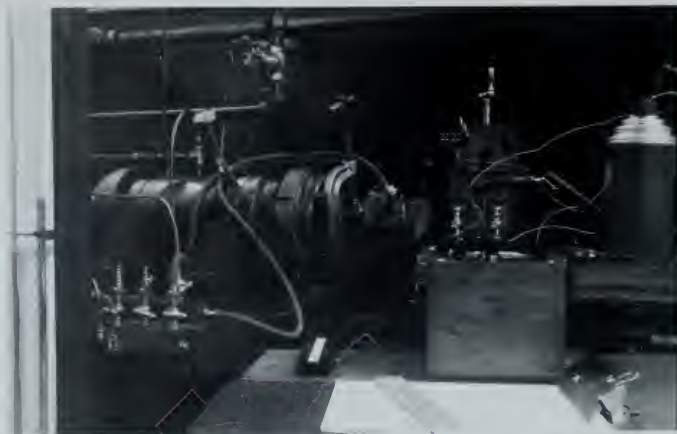
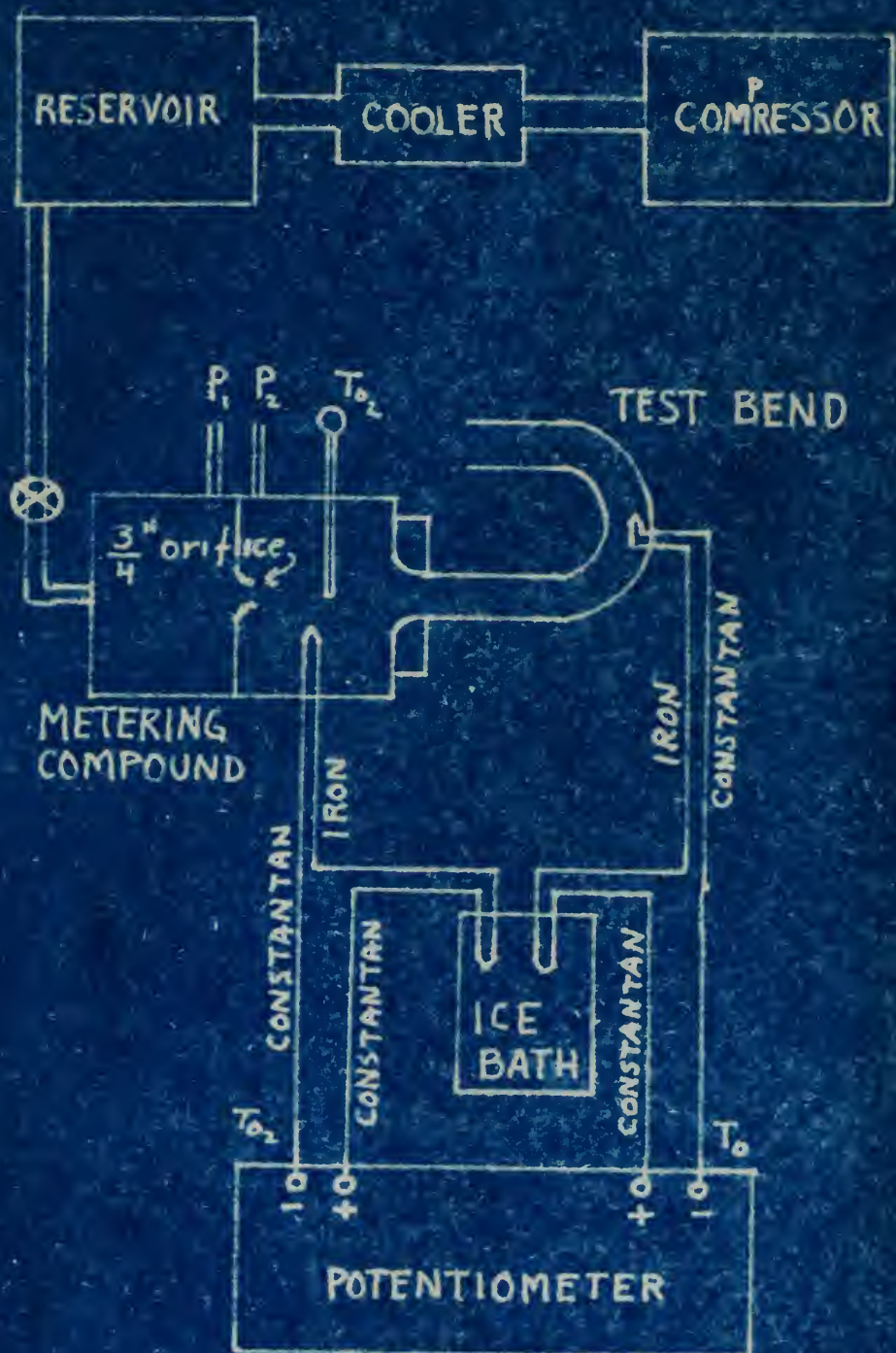


FIGURE 2





SCHEMATIC OF TEST EQUIPMENT.  
FIGURE 3.

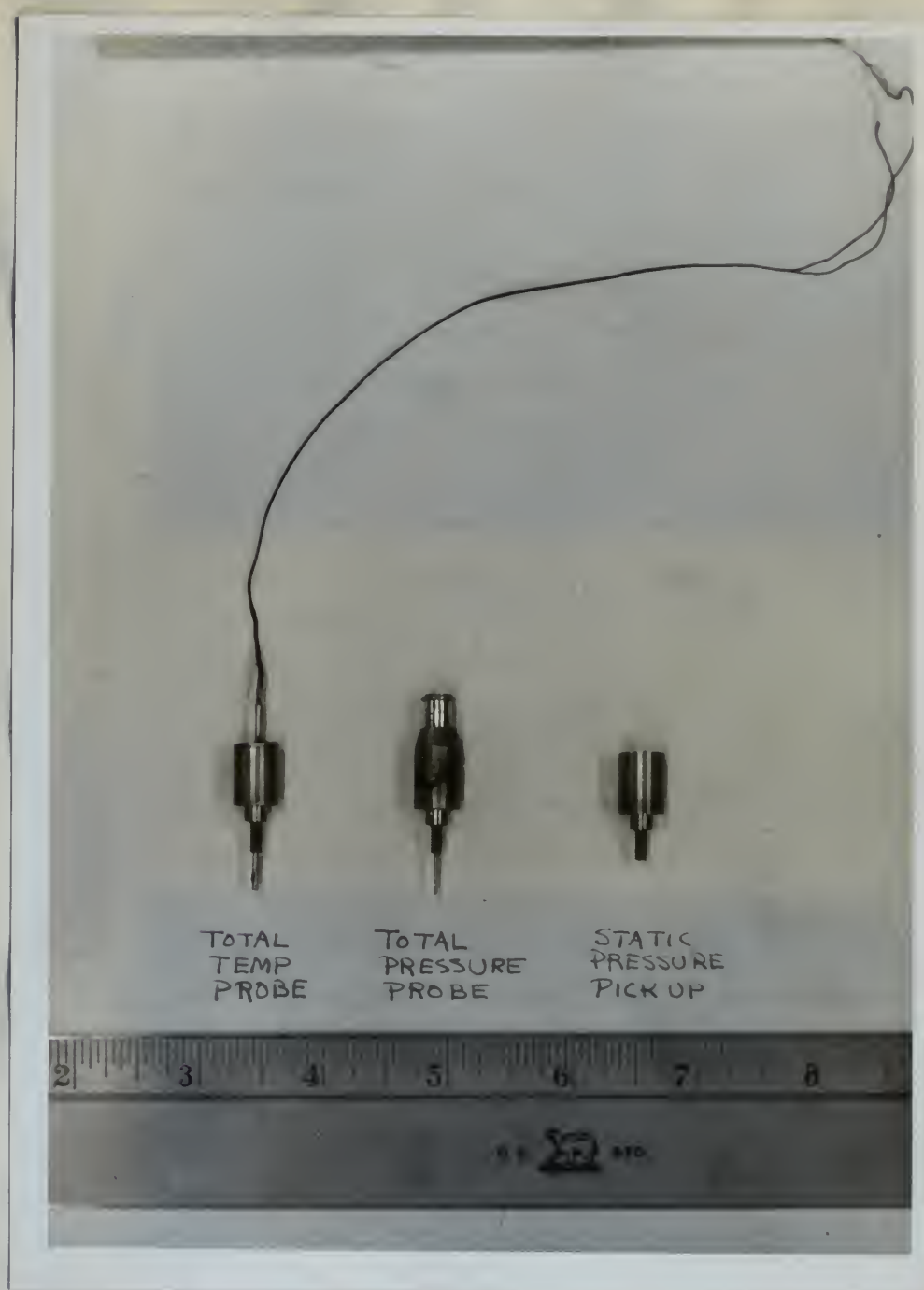


FIGURE 4



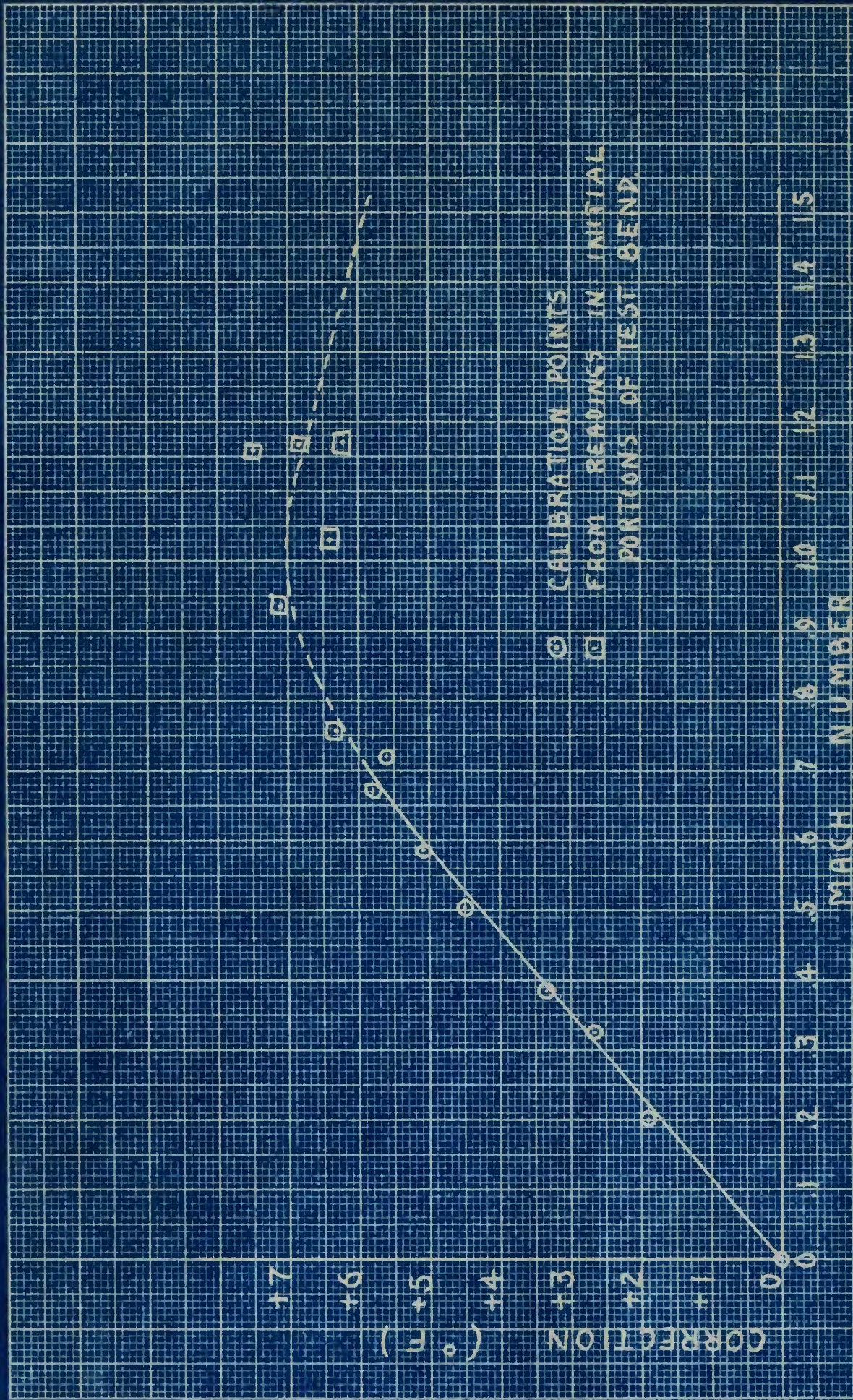


FIGURE 5 - IMPACT TEMP. CORRECTIONS.





FIGURE 6A



FIGURE 6B



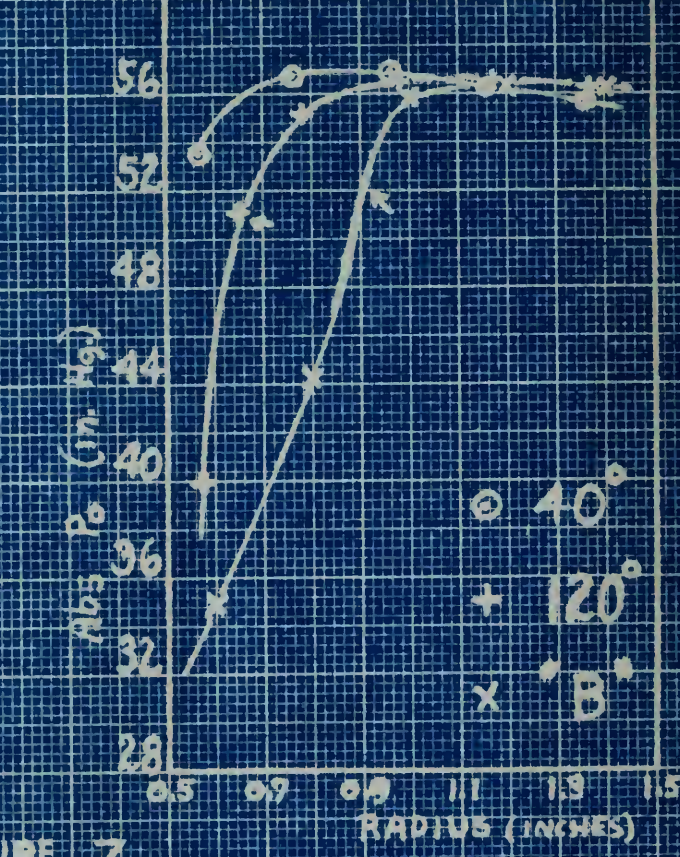
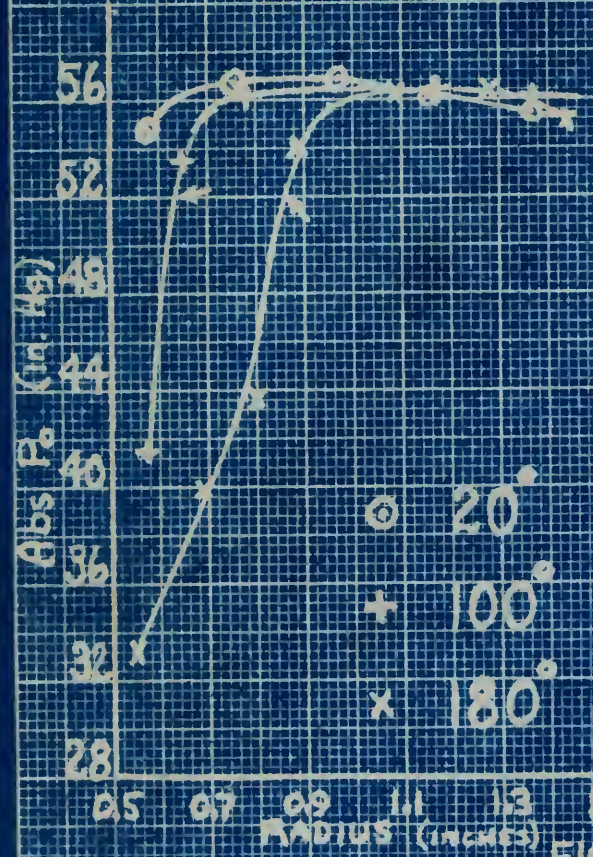
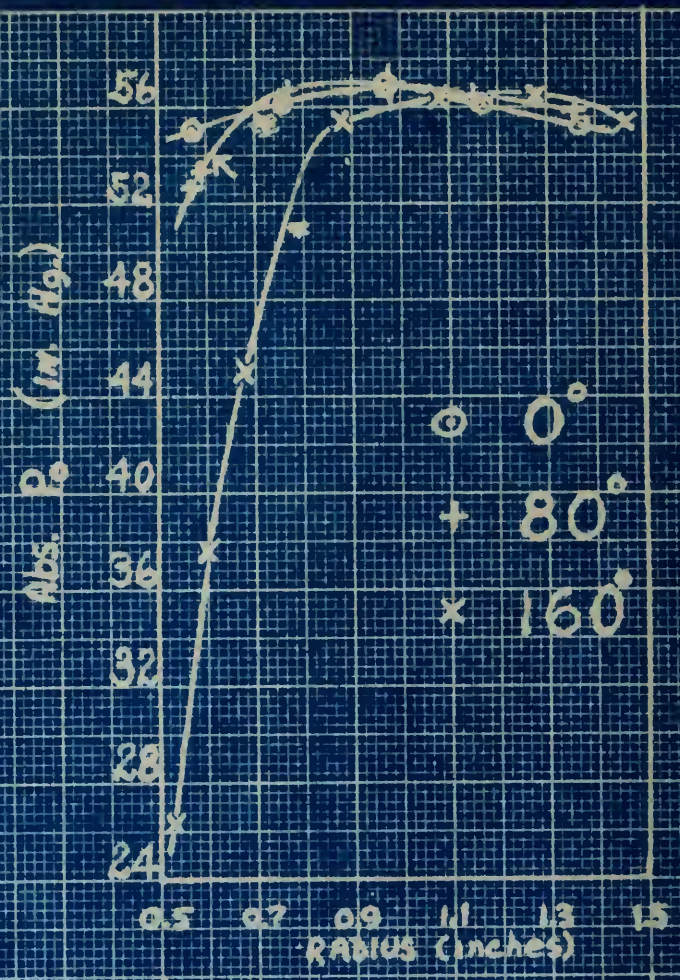
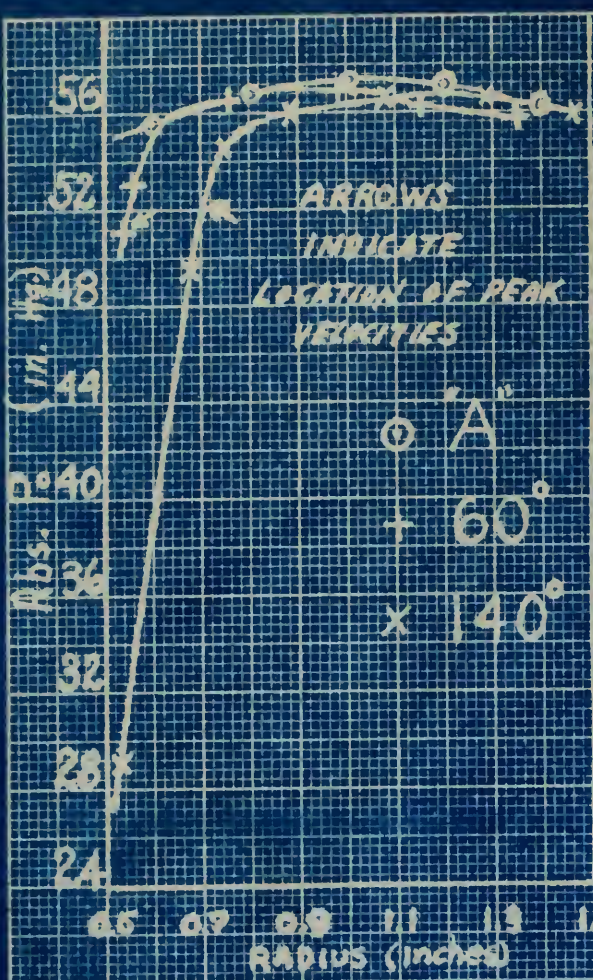
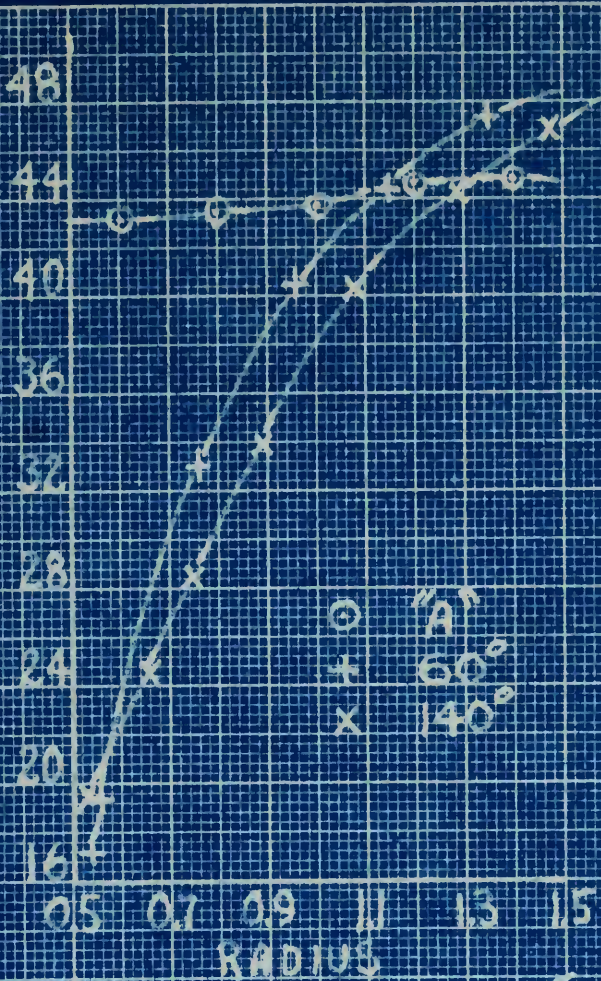


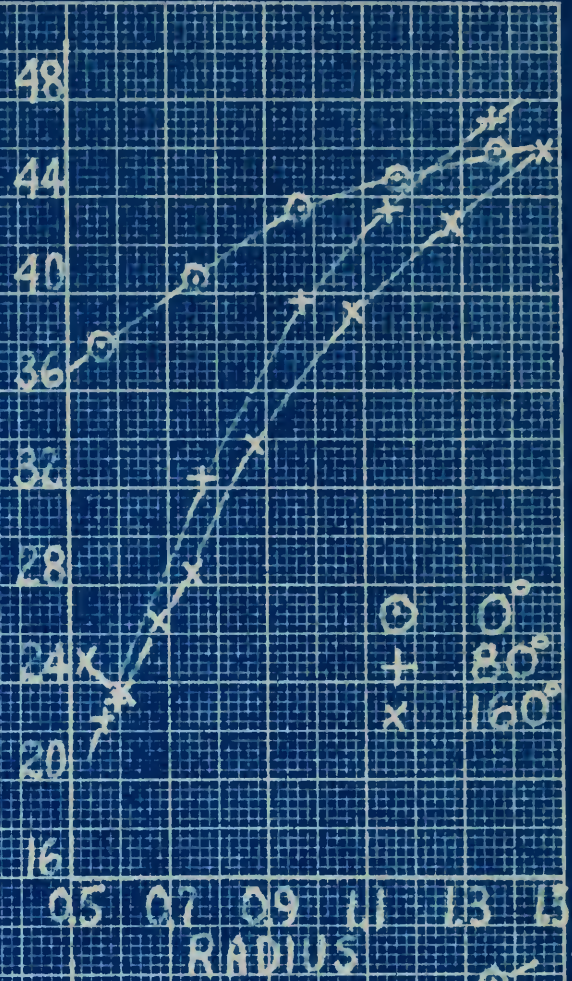
FIGURE 7  
ABSOLUTE TOTAL PRESSURE VS RADIUS



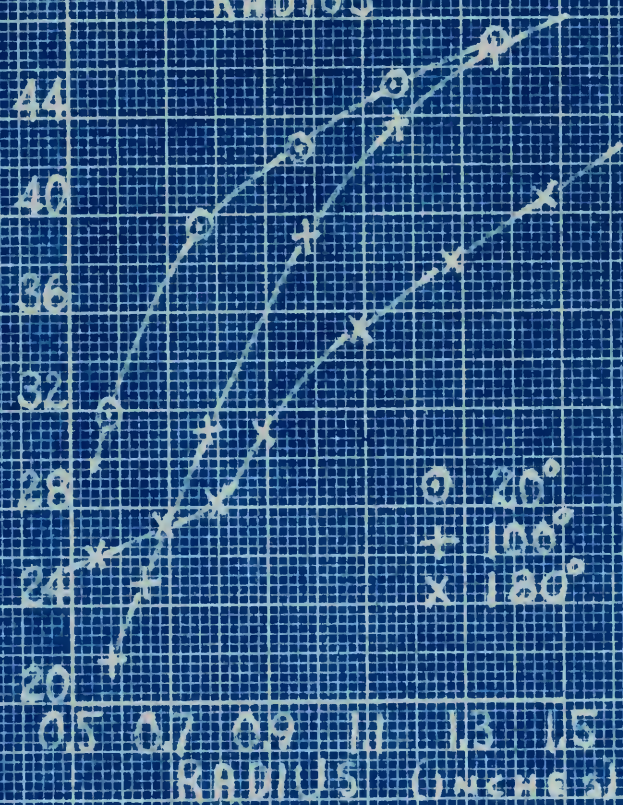
STATIC PRESSURE (INCHES MERCURY ABS.)



STATIC PRESSURE (INCHES MERCURY ABS.)



STATIC PRESSURE



STATIC PRESSURE

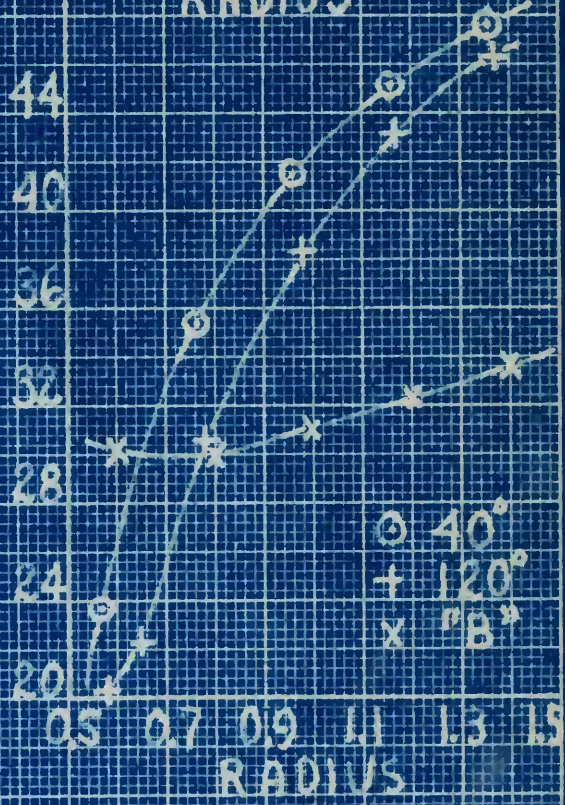


FIGURE 8

ABSOLUTE STATIC PRESSURE VS. RADIUS.



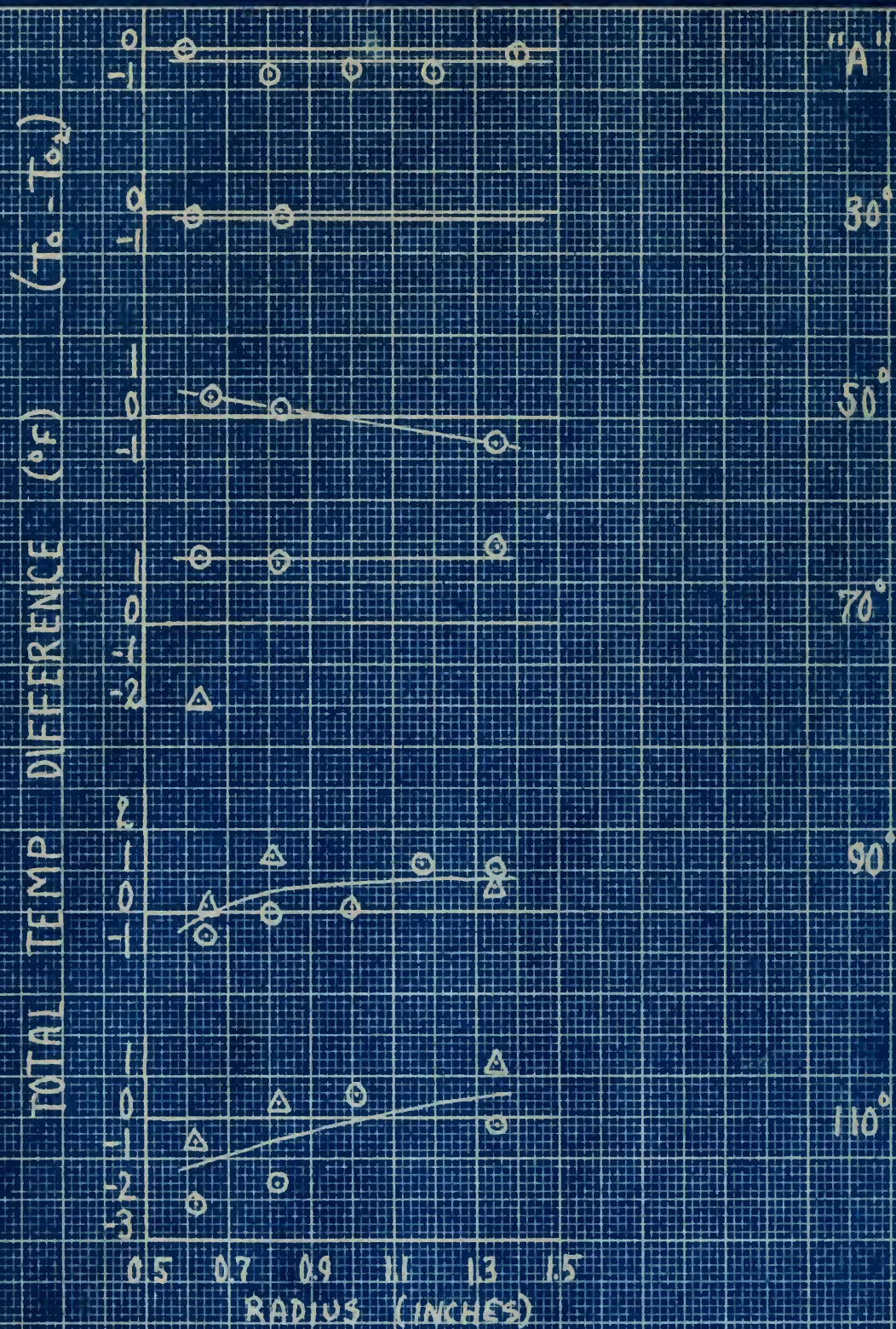


FIGURE 9a

TOTAL TEMPERATURE DIFFERENCE  
VS  
RADIUS.



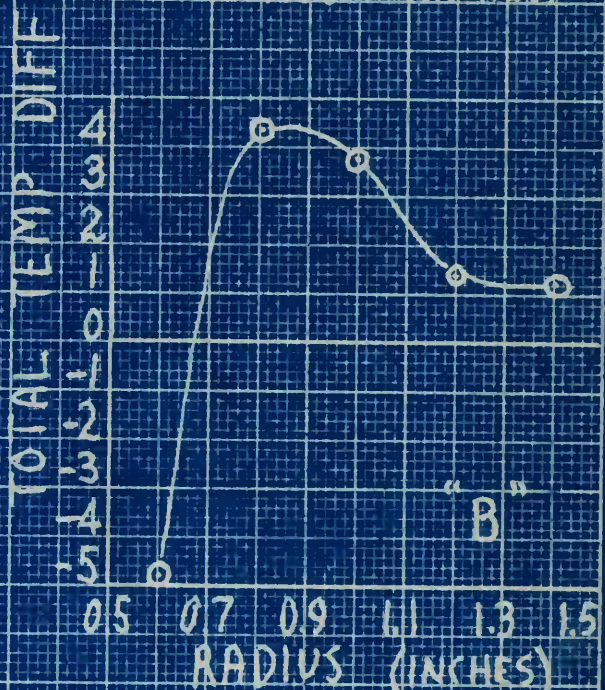
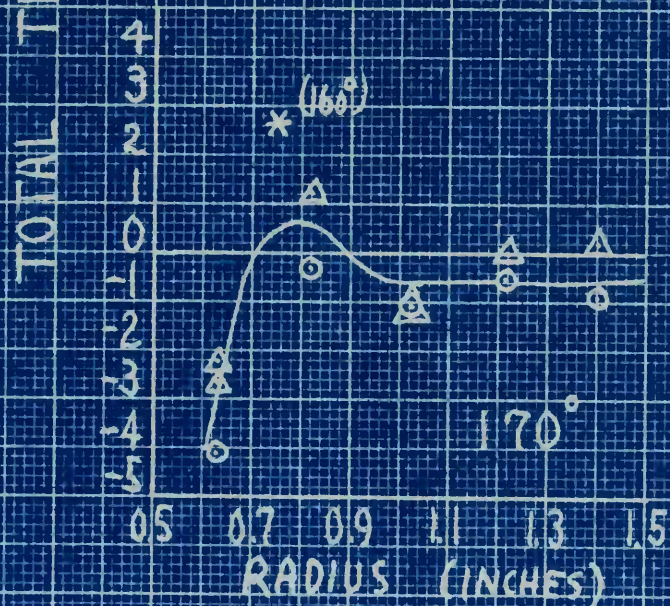
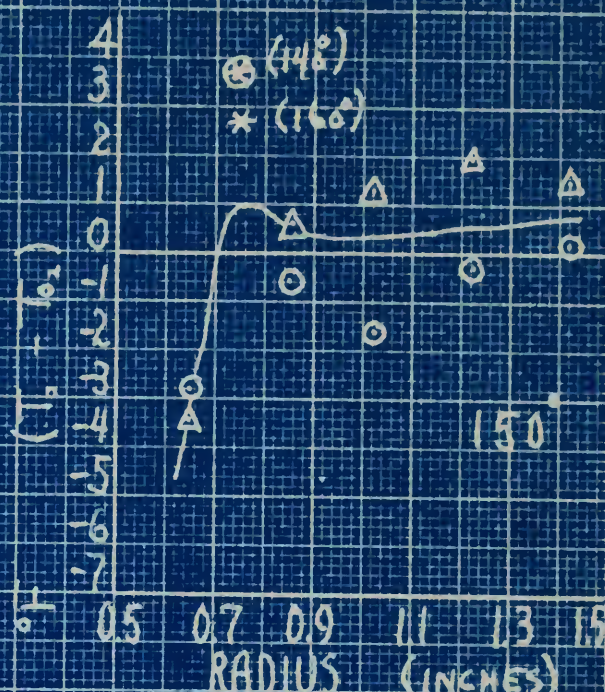
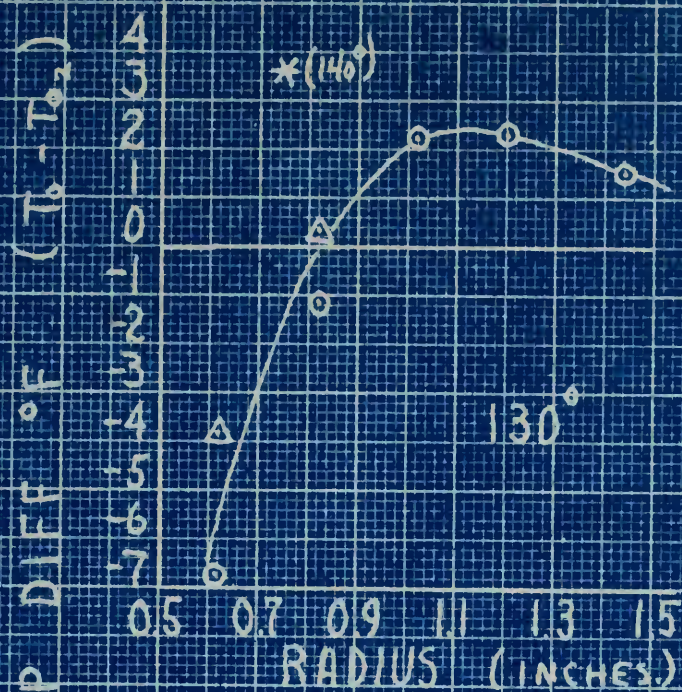


FIGURE 9 B  
TOTAL TEMPERATURE DIFFERENCE  
VS  
RADIUS.



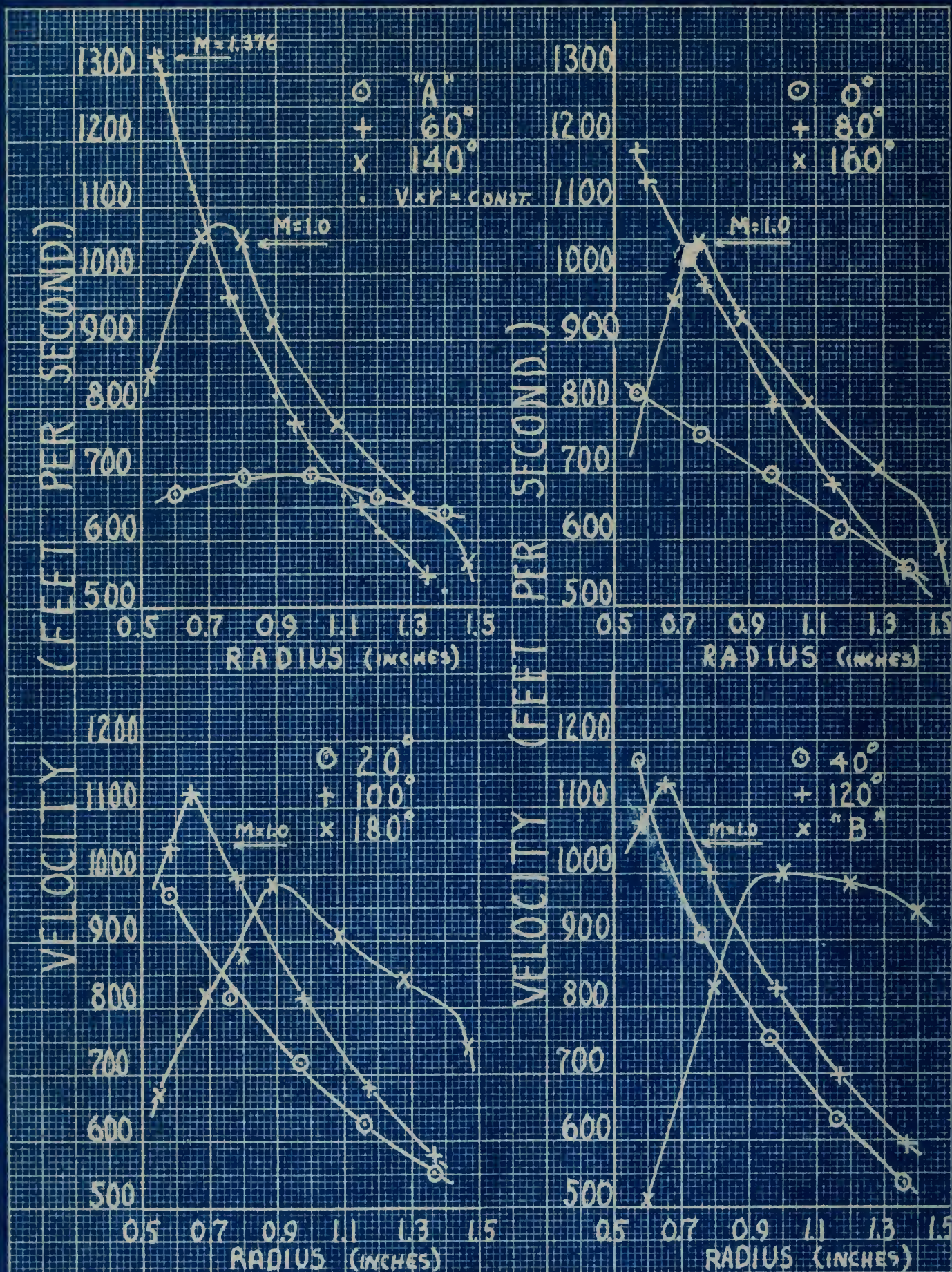


FIGURE 10 - VELOCITY vs RADIUS.



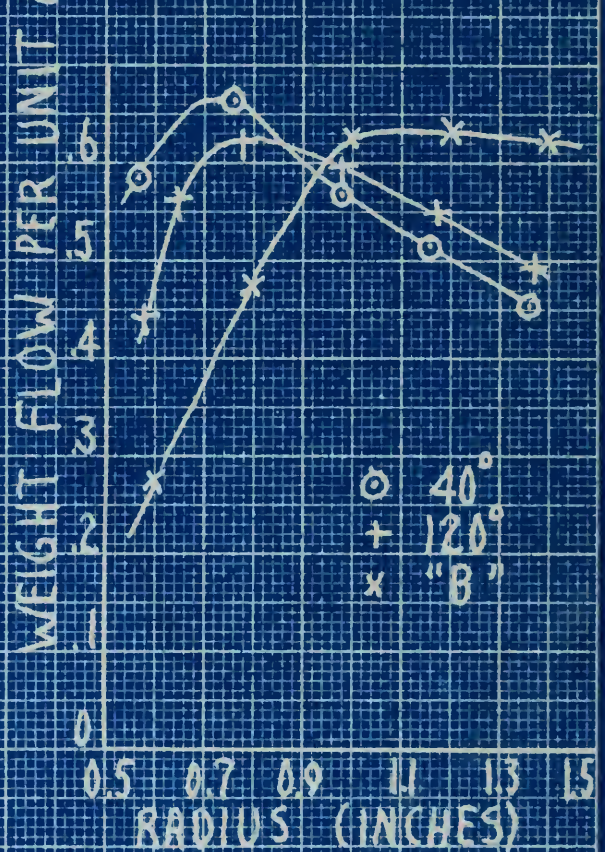
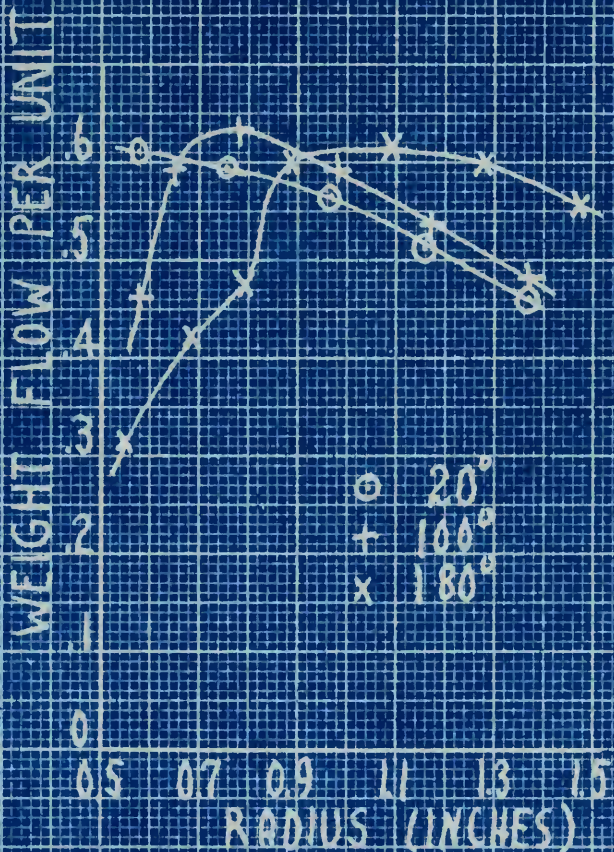
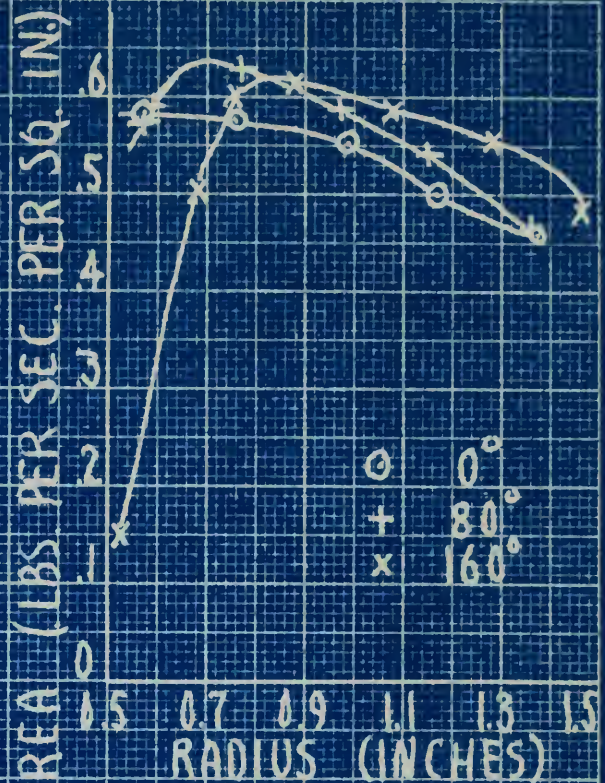
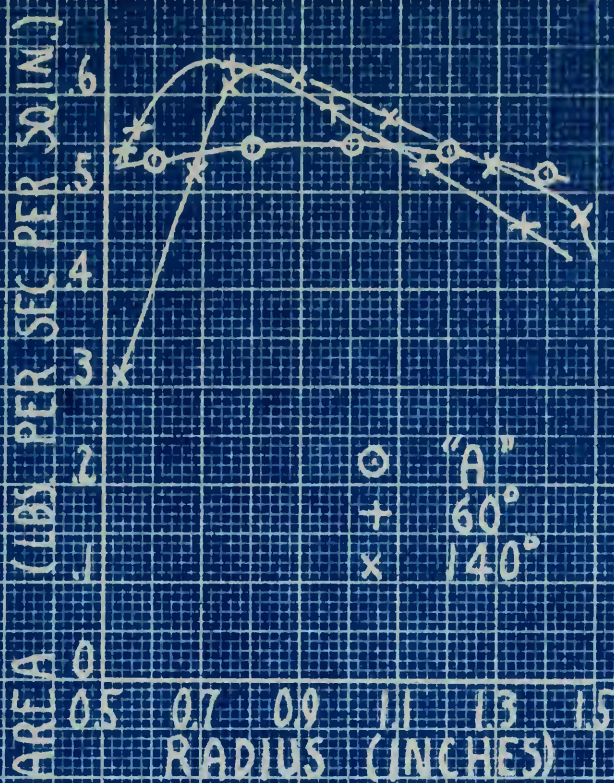


FIGURE 11.  
WEIGHT FLOW PER UNIT AREA  
VS  
RADIUS



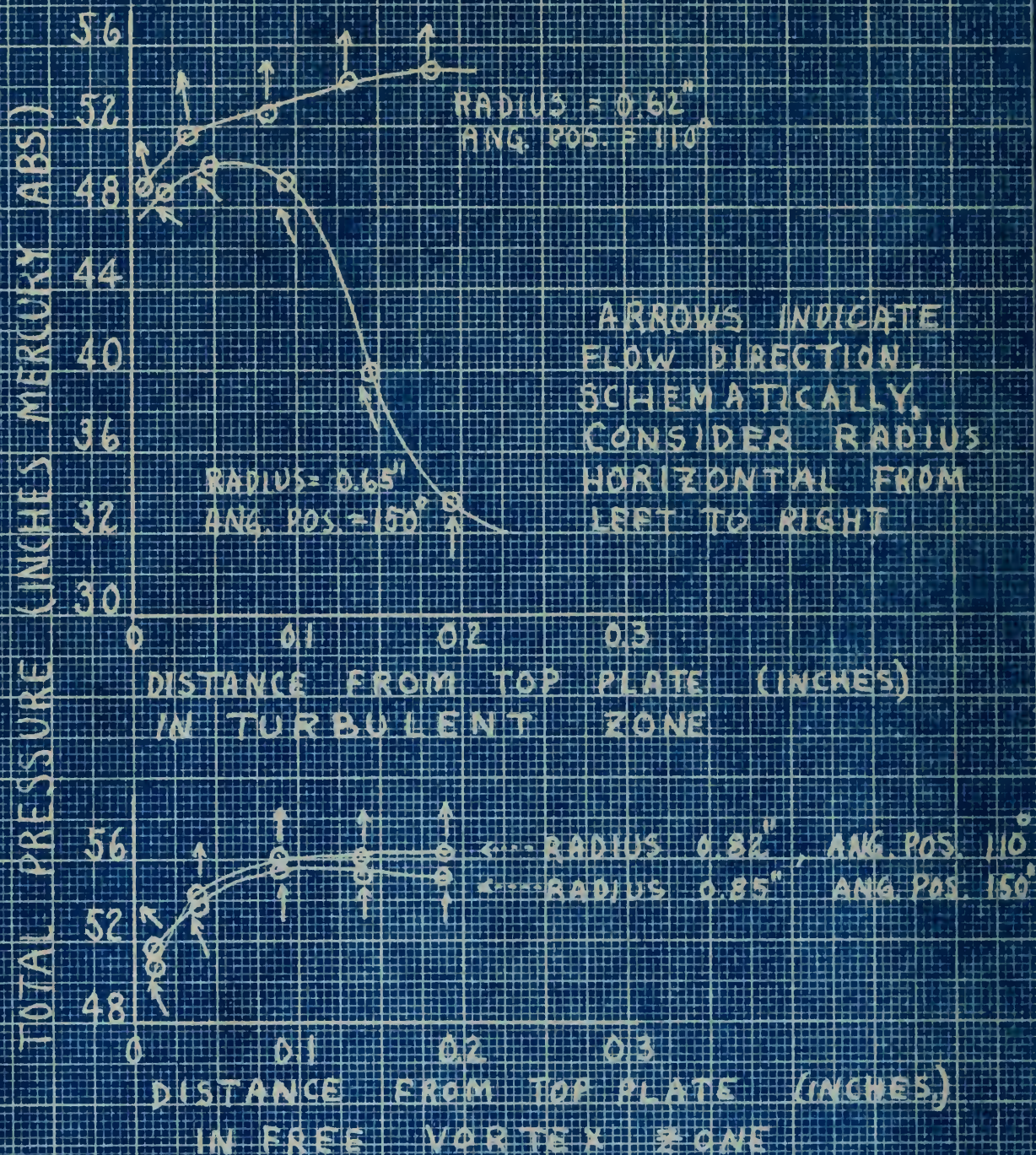


FIGURE 12.

TOTAL PRESSURE VARIATIONS  
IN THE VERTICAL TO THE  
PLANE OF CURVATURE



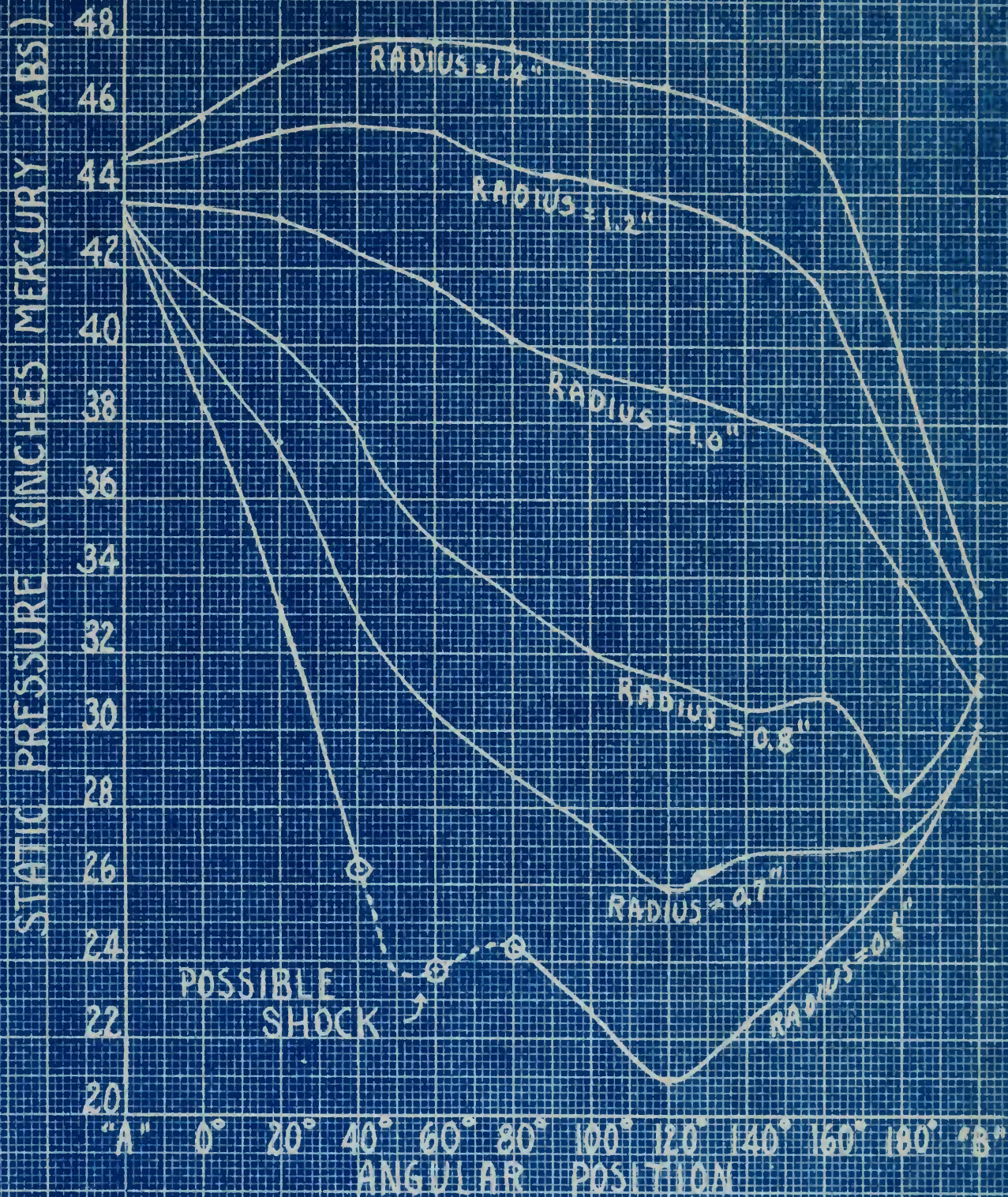


FIGURE 13.  
 STATIC PRESSURE  
 vs  
 ANGULAR POSITION



## DATE DUE

[illegible]

Thesis

11258

M83

Morrison

An investigation of  
high velocity air flow  
in a bend.

Thesis

11258

M83

Morrison

An investigation of  
high velocity air flow  
in a bend.



PRESS BINDER

BGS 2507

MADE BY

PRODUCTS, INC.

ENSBURG, N. Y.



thesM83

An investigation of high velocity air fl



3 2768 001 91712 3

DUDLEY KNOX LIBRARY